PLANT SCIENCE TODAY
ISSN 2348-1900 (online)
Vol 9(2): 345–356
https://doi.org/10.14719/pst.1449

HORIZON
e-Publishing Group
HePG

RESEARCH ARTICLE

Phytofabrication of gold and bimetallic gold-silver nanoparticles using aqueous extract of wheatgrass (*Triticum aestivum* L.), their characterization and assessment of antibacterial potential

Vikas Pahal[1*], Pankaj Kumar[2], Parveen Kumar[3] & Vinod Kumar[4]

[1]Department of Microbiology, Dolphin (P.G) College of Science and Agriculture, Chunni Kalan, F.G. Sahib, Punjab, India
[2]Department of Microbiology, Dolphin (P.G) Institute of Biomedical and Natural Sciences, Manduwala, Dehradun, Uttarakhand, India
[3]Bio-Nanotechnology Lab, Division: H-1, Central Scientific Instruments Organization (CSIO), Chandigarh (U.T), India
[4]HR-TEM Facility Lab, National Institute of Pharmaceutical Education and Research (NIPER), SAS Nagar, Punjab, India

*Email: vikaspahal3@gmail.com

OPEN ACCESS

ARTICLE HISTORY
Received: 25 July 2021
Accepted: 06 January 2022

Available online
Version 1.0 (Early Access): 20 February 2022
Version 2.0: 01 April 2022

Additional information

Peer review: Publisher thanks Sectional Editor and the other anonymous reviewers for their contribution to the peer review of this work.

Reprints & permissions information is available at https://horizonepublishing.com/journals/index.php/PST/open_access_policy

Publisher's Note: Horizon e-Publishing Group remains neutral with regard to jurisdictional claims in published maps and institutional affiliations.

Indexing: Plant Science Today, published by Horizon e-Publishing Group, is covered by Scopus, Web of Science, BIOSIS Previews, Clarivate Analytics, etc. See https://horizonepublishing.com/journals/index.php/PST/indexing_abstracting

CITE THIS ARTICLE

Pahal V, Kumar P, Kumar P, Kumar V. Phytofabrication of gold and bimetallic gold-silver nanoparticles using aqueous extract of wheatgrass (*Triticum aestivum* L.), their characterization and assessment of antibacterial potential. Plant Science Today 9(2): 345–356. https://doi.org/10.14719/pst.1449

Abstract

In the present study, gold (AuNPs) and gold-silver bimetallic nanoparticles (Au-Ag BMNPs) were fabricated by using aqueous leaf extract of *Triticum aestivum* L. - a crop plant, and their bactericidal potency was checked against selected pathogenic bacterial strains. The phytofabricated AuNPs and BMNPs were analyzed for their physical attributes using UV–Visible and Fourier transformed infrared spectroscopy (FTIR), Dynamic light scattering (DLS), High-resolution transmission electron microscopy (HRTEM), and Energy-dispersive X-ray spectroscopy (EDX). Bactericidal efficiency of synthesized NPs was evaluated using agar-well diffusion and XTT (2,3-Bis-(2-Methoxy-4-Nitro-5-Sulfophenyl)-2H-Tetrazolium-5-Carboxanilide)-colorimetric assays against *Klebsiella pneumoniae*, *Salmonella typhimurium*, *Enterobacter aerogenes*, *Escherichia coli*, *Micrococcus luteus*, *Staphylococcus aureus*, *Streptococcus mutans* and *Staphylococcus epidermidis*. HRTEM analysis revealed that both kinds of nanoparticles (NPs) were highly crystalline in nature and of spherical to oval-shaped. AuNPs size was found in the range of 5-40 nm, whereas BMNPs showed their size in the range of 5-30 nm. HRTEM results were corroborated by DLS results which revealed the average hydrodynamic diameter of AuNPs and BMNPs in the range of 29.08 and 26.56 nm respectively. UV-visible spectroscopy showed high-intensity single spectral peaks at 540 and 480 nm for AuNPs and BMNPs respectively. FTIR analysis demonstrated that protein, flavanones, hydroxyl, carboxylate groups and reducing sugars were responsible for reducing and capping of both NPs. *K. pneumonia* and *S. typhimurium* were found to be the most sensitive bacteria towards BMNPs-mediated (MIC: 400 µg/ml) and AuNPs-mediated toxicity (MIC: 800 µg/ml). It was observed that BMNPs generally possessed more powerful bactericidal effect against all bacterial strains in comparison to AuNPs. Minimum inhibitory concentration (MIC) and Minimum bactericidal concentration (MBC) values were observed in the concentration range of 400 µg/ml-1.5 mg /ml for different bacterial strains. Furthermore, it was demonstrated that phytosynthesized AuNPs have their own bactericidal effect, but at higher concentrations (>100 µg/ml) and bactericidal effect of BMNPs was due to the synergistic effect of both Ag and Au ions, which was also observed to be dose-dependent.

Keywords

AuNPs, Ag-Au BMNPs, bactericidal effect, NPs, XTT-colorimetric assay

Introduction

Nanometer-sized particles of different metals have revolutionized and opened novel avenues in diverse fields owing to their enhanced physico-chemical properties with respect to their bulk materials (1, 2). Nobel metals like, gold nanoparticles (also known as colloidal gold) attract the attention of researchers due to their inherent superior physico-chemical characteristics like high surface area, chemically inertness (resistance to oxidation), higher stability in comparison to other metallic nanoparticles (NPs), enhanced biocompatibility and non-cytotoxicity to human cells and tissues. These aforementioned properties resulted in their tremendous applications in the field of medicine and other related fields such as magnetic, optical, electronic, catalytic (3, 4), bio-imaging, nano-biosensing, probes and markers, targeted drug delivery (5), photo-hyperthermia, water remediation, genetic engineering, diagnosis and therapeutics (6, 7).

Similarly, in recent times bimetallic nanoparticles (especially Ag-Au BMNPs) have attracted attention as a new enhanced version of designer-nanoparticles because of their unique and distinct properties which are superior to their ingredient metallic NPs (Ag or Au). These bimetallic NPs possessed appreciably enhanced therapeutic efficiency compared to their individual metals by retaining the biocompatibility and stability of AuNPs and decreasing the level of toxicity of AgNPs toward human cells (8). Furthermore, the synergistic effects of both Ag and Au NPs in a bimetallic body have countless applications in various fields like optoelectronics, sensors, agriculture, disease and toxin biomarkers (9, 10), magnetic, antimicrobial, environmental monitoring, catalysis and aptamer-based nanosensors (9, 11-13).

Various chemical, physical and hybrid methods were defined in literature for the fabrication of AuNPs and bimetallic (BMNPs) Ag-Au NPs like hydrothermal, reverse micelle, ion-sputtering, sol-gel, chemical reduction, γ-irradiation, laser ablation, microwave irradiation, ultraviolet radiation, thermolytic process, photochemical process, sonochemical method etc. (12, 13). The limitations of these methods are that they are quite expensive and unfortunately hazardous to both environment and biological tissues because of their toxic by-products which have a direct effect on their biocompatibility. Synthesis of nanoparticles by environment-friendly and cost-effective processes is one of the vital aspects of current nanotechnology research (14). Hence, the synthesis of NPs *via* biogenic sources like bacteria, fungi (15, 16), green algae (17), plants or plant-based products like starch, cellulose, enzymes or phytochemicals (1, 2, 7, 18) has garnered significant attention since last decade. Out of these biogenic methods, plant-based methods are relatively more versatile, simple, fast, eco-friendly, less tedious, less time consuming, non-harmful, non-immunogenic, relatively reproducible, environmentally benign and free of microbial originated contaminations (19). Moreover, phytocomponents acts as both capping and reducing agents in the biosynthesis of NPs (11, 18).

Indiscriminate and overuse of antibiotics and paucity of new and effective antibiotics have led to a post-antibiotic era with an increased number of mortality and morbidity cases due to proliferation of resistant pathogenic bacterial strains (20, 21). Since the beginning of this problem, the scientific community worldwide engaged in developing new and potentially effective antibacterial agents having no or minimum side effects (22). As per various reports, developing the novel bactericidal agent with profound specific effect and minimum or no side effects to body tissues is currently recognized as one of the top-most priorities in medical research (14). Different metallic NPs were synthesized and used as antimicrobial agents like zinc, silver, copper, magnesium, silver and gold (22). Among these NPs, silver nanoparticles were found to be the most potent antimicrobial agents along with undesirable properties like harmful effect on healthy body tissues, prone to fast oxidation and less stability in body fluids which ultimately limited their use as an antimicrobial agent. So, both AuNPs and Ag-Au NPs have received substantial consideration due to their excellent bactericidal potency and simultaneously absence of any aforementioned side effects of AgNPs.

In literature, there has been ambiguity with regard to the bactericidal potency of AuNPs. Similarly, in the case of Au-Ag bimetallic nanoparticles (BMNPs), the ambiguity is whether the bactericidal effect is due to the silver ions or gold ions, or is due to their synergistic effect ? It has been claimed that this ambiguity in bactericidal potential of AuNPs/BMNPS is may be due to the reason that different authors used different materials and methodologies for their fabrication. In the present research, phytofabrication of both AuNPs and Au-Ag BMNPs were performed using bottom-up approach under same standard conditions of temperature, pH, purification methods, concentration of precursor salts and reducing agent. Reducing and capping agent was aqueous extract of two weeks long leaflets of wheatgrass (*Triticum aestivum*), a crop plant. Water extract of *Triticum aestivum* is known as “green-blood” and has been found to possess flavonoids, phenolics compounds, lignins, alkaloids, tannins, vitamins, terpenoids, amino acids, carbohydrates and protein and also reported to have anti-inflammatory, immune-modulatory, antioxidant and antibacterial activities (23, 24). These synthesized NPs were analyzed for their physical attributes and evaluated further for their bactericidal efficiency against same experimental bacterial strains using agar-well and XTT-colorimetric assays to answer these above-mentioned ambiguities in literature.

Materials and Methods

HD 2967 variety of wheat is very common in Punjab area and same was grown in our agriculture-laboratory for phytofabrication of NPs. Silver nitrate ($AgNO_3$), menadione, hydrogen tetrachloroaurate ($HAuCl_4.XH_2O$), sodium salt of XTT were procured from Sigma Aldrich, Chandigarh (U.T), India and used without further purification. MHB (Muller Hinton Broth) and MHA (Muller Hinton Agar), sodium hy-

droxide (NaOH) and HPLC purified water were purchased from HiMedia chemicals, Chandigarh (U.T), India. All the solutions and reagents were prepared in HPLC purified water.

Phytofabrication of AuNPs and BMNPs

Phytofabrication is a process which involves reduction of metallic salts into their respective NPs with the help of aqueous extract of plants. Leaves of two weeks long plant *Triticum aestivum* L. (Wheatgrass) were adequately washed, dried (pressed between folds of filter paper) and chopped into smaller pieces. Approximately, 20 g of chopped leaves were crushed with blender grinder and the resulted pulverized material was mixed with 100 ml HPLC purified water. The solution was boiled for 10 min at 90+1 ^{0}C and then cooled at room temperature. After that, the extract was first filtered through Whatman filter paper (1) and followed by centrifugation for 7-8 minutes at 8000 rpm to remove any remaining plant-debris or impurities. This extract was used for the fabrication of both AuNPs and BMNPs (5, 18).

For the biosynthesis of AuNPs, 1mM hydrogen tetrachloroaurate ($HAuCl_4.XH_2O$) solution was prepared, and in case of bimetallic NPs (Ag-Au BMNPs), 1 mM $AgNO_3$ (pH 4.29) and 1mM gold chloroaurate (pH 2.29) solutions were mixed in 1:1 volume ratio (pH 5.31). For the phytofabrication of NPs, 10 ml hot plant-extract was added into two different 250 ml capacity Erlenmeyer flasks one containing 90 ml 1mM hydrogen tetrachloroaurate ($HAuCl_4.XH_2O$) and other containing 90ml of mixed solution (1 mM $AgNO_3$ and 1mM gold chloroaurate solution in 1:1 volume ratio) with constant stirring on a magnetic stirrer by maintaining the temperature at 90+1 ^{0}C for 8-10 min. The pH of both the reaction solutions was maintained at 10.0+0.2 with the help of 1M NaOH. This resulted in the reduction of metallic salts (simultaneous co-reduction of both salts in case of BMNPs), and within 10-15 seconds, the colour of solutions turned to ruby red and violet-blue which indicates the formation of AuNPs and BMNPs respectively (8, 18). Both the solutions were then incubated for 4-5 hrs. at room temperature. After that incubation, solutions were centrifuged for 10-15 min at 16000 rpm, followed by removing supernatant from the settled NPs. This procedural step was reiterated thrice with HPLC purified water. At last, NPs were dissolved in HPLC purified water and dried in a vacuum oven at 50 ^{0}C in a petridish. AuNPs and BMNPs were collected as a dry powder and analyzed further for their physical and bactericidal properties.

Characterization of NPs

UV-visible and FTIR spectroscopy

Synthesis of AuNPs and BMNPs (Ag-Au NPs) were confirmed by scanning the absorption maxima of both AuNPs and BMNPs using UV-visible spectrophotometer (Thermo Fisher Scientific, India) in the wavelength range of 300–700 nm. The FTIR analysis was determined with FTIR spectrometer (Perkin Elmer) at a resolution of 4 cm^{-1} in the wavelength range of 4000–250 cm^{-1} (5, 8, 18). The obtained FTIR spectra were plotted as absorbance (%) versus wavenumber (cm^{-1}).

DLS

The hydrodynamic diameter of both AuNPs and BMNPs in suspen-sion was determined using DLS method (8, 18). In this experiment, the aqueous suspension of the synthesized AuNPs and BMNPs was first percolated through a filter unit (0.22 µm), and then the hydrodynamic diameter of both NPs was measured by using Malvern Zetasizer Nanosystem (Worcestershire, U.K).

HRTEM and EDX

Topographical properties of both AuNPs and BMNPs were determined by HRTEM microscopy using the standard protocol of analysis (25). A drop of synthesized NPs solution was placed on a copper grid (carbon-coated) of HRTEM followed by blotting the excess solution at room temperature after 3-4 min. The grids were analyzed with the help of FEI TECNAI (G2 F20) system at 200 keV. HRTEM micrographs were produced at 6 $X10^6$ times magnification and with 0.2 A^0 resolutions. The elemental composition of synthesized nanoparticles was characterized using EDX microanalysis in EDX spectroscopy associated with HRTEM.

Assessment of bactericidal activity of AuNPs and BMNPs

Test microorganisms

Four gram-negative bacterial strains *Klebsiella pneumoniae* (MTCC 432), *Salmonella typhimurium* (MTCC 3224), *Enterobacter aerogenes* (MTCC 2824), *Escherichia coli* (MTCC 443) and 4 gram-positive bacterial strains *Micrococcus luteus* (MTCC106), *Staphylococcus aureus* (MTCC 3160), *Staphylococcus epidermidis* (MTCC 9040) and *Streptococcus mutans* (MTCC 890) were procured from IMTECH (Institute of Microbial Technology), Sector 39, Chandigarh (U.T), India as reference strains to check the antibacterial potential of synthesized AuNPs and BMNPs.

Antibacterial assays

Bactericidal potency of synthesized AuNPs and BMNPs against pathogenic bacterial strains was checked using standard agar-well diffusion and XTT-colorimetric assays. Prior to the respective assays, concentrations of all bacteria strains were standardized (26, 27). Briefly, overnight cultured bacterial strains were re-cultured in MHB at 37 ^{0}C for 2-3 hrs. These midlogarithmic phase microorganisms were then centrifuged for 10-12 min (4 ^{0}C) at 4,000 rpm. The obtained bacterial pellets were washed 2 to 3 times with 10 mM sodium phosphate buffer (pH=7.4). Optical density (O.D) of respective bacterial aliquot was calculated at 620 nm, and the concentrations of bacteria were standardized for 5 x 10^7 colony-forming unit/ml (OD_{620}:0.20). This standardized concentration of bacteria was used in both agar-well diffusion and XTT-colorimetric assays.

Agar-well diffusion Assay

In this experiment, 100 µl of standardized concentration of respective bacteria (5 x 10^7 colony-forming unit/ml) was uniformly seeded on sterilized MHA plates using sterile J-shaped glass-rod (27). After 30 min, wells were made in MHA plates aseptically. The resulted wells were loaded with 90 µl of different concentrations of AuNPs and BMNPs. After that, the plates were incubated at 37 °C for 24 hrs. The assay was repeated thrice, and the antibacterial potential of

AuNPs and BMNPs was measured as ZOI (zone of inhibition) around the well in mm scale (mean + standard deviation). In this experiment, if the ZOI was observed to be less than or equal to 0.5 mm, then it was considered as "No bactericidal effect" for that specific concentration of NPs.

XTT-colorimetric assay

Generally, the agar-well diffusion method is used for primary screening which gives a rough estimate of bactericidal efficiency of NPs or other inhibitory molecules. There are certain limitations of the agar-well approach like: a.) agar produces hindrance in free movement of nanoparticles, b.) have a direct effect on the release of silver or gold ions (Ag^{+}/Au^{+3}) from the surface of NPs, and c.) absence of optimum contact between bacteria and NPs, which is necessary for an accurate evaluation of bactericidal effect (25, 29). The XTT salt-based colorimetric method is a gold standard in the assessment of the bactericidal effect of NPs, because this method is devoid of all the limitations of agar-well method as discussed above (27, 28, 30). This method measured the water-soluble formazan at 490 nm, which was produced due to reduction of XTT salt by the dehydrogenase enzyme of metabolic active bacterial cells. Change in absorbance value of formazan can be correlated to cell viability (30).

In this experiment, 170µl broth of the standardized bacterial concentration (5 x 10^{7} CFU/ml) was poured into 96 -well flat-bottom plate, followed by addition of 30 µl of different concentrations of AuNPs and BMNPs with gentle mixing. The plates were then incubated for 14-16 hrs at 37 ^{0}C. After incubation, 100 µl of the reaction mixture from the incubated plates was aseptically transferred into a new plate followed by addition of 25 µl of fresh XTT (0.5 mg/ml) +menadiaone (1 mM) solution (12.5:1 v/v ratio) with gentle mixing. The flat-bottom plates were further incubated in the dark for 2 hrs at 37 °C and the change in absorbance value of formazan was calculated with the help of microplate reader (Thermo Fisher Scientific, India) at 490 nm. Muller-Hinton broth with respective bacterial strains and without any inhibitor acts as a negative control. This experiment was performed in triplicate, and the final readings were taken after subtracting the readings of specific blanks. Antibacterial efficacy was calculated as follows:

$$\text{Percentage reduction (\% Rd)} = 100\% - \left[\frac{(\text{well absorbance} - \text{Blank absorbance}) \times 100}{\text{Negative control absorbance}}\right]$$

In this experiment, if the percentage reduction was observed to be less than 5%, then it was considered as "No bactericidal effect" for that specific concentration of NPs. Antibiotic ciprofloxacin (0.5 mg/ml) was used as a positive control in both the above-discussed experiments (27).

Assessment of MIC and MBC values

MIC values for each test bacteria were evaluated on the basis of results obtained in XTT-colorimetric assay. The lowest concentration of NPs that restricted bacteria's growth completely as established by the XTT-colorimetric results was considered MIC value for that particular bacterial strain. MBC values were evaluated by sub-culturing the 100 µl preparations from the selected tubes (that did not show any bacterial growth as per XTT-colorimetric results) over the MHA plates and their subsequent incubation at 37 °C for 24 hrs. The lowest concentration of NPs, which completely inhibited the bacterial growth on antibiotic-free MHA-media, was considered the MBC value of that particular bacterial strain (27).

Results

The colour of the reaction mixture changed from colourless to ruby red (AuNPs) and to violet-blue (Ag-Au BNPs) within 10-15 seconds was due to the SPR (surface plasmon resonance) effect which indicated the completion of reduction reactions.

UV-Visible spectroscopy results

UV-Vis spectra of AuNPs and Ag-Au BMNPs showed an absorption peak maxima at wavelength 540 nm and 480 nm respectively (Fig. 1A & 2A).

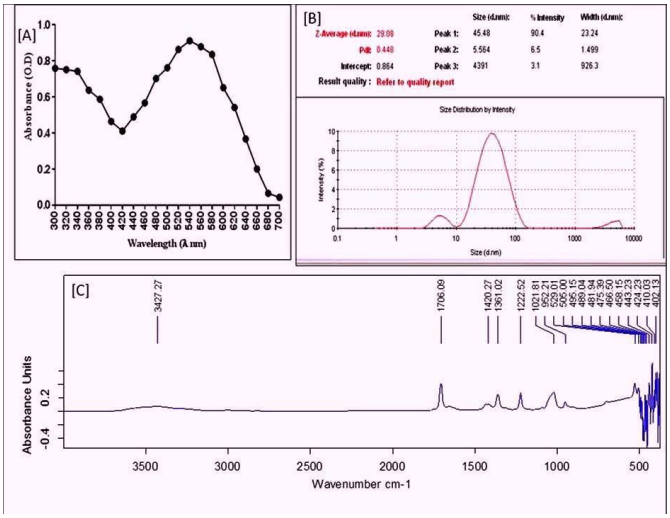

Fig. 1. UV-Vis [**A**]; DLS [**B**] and FTIR [**C**] spectra of AuNPs

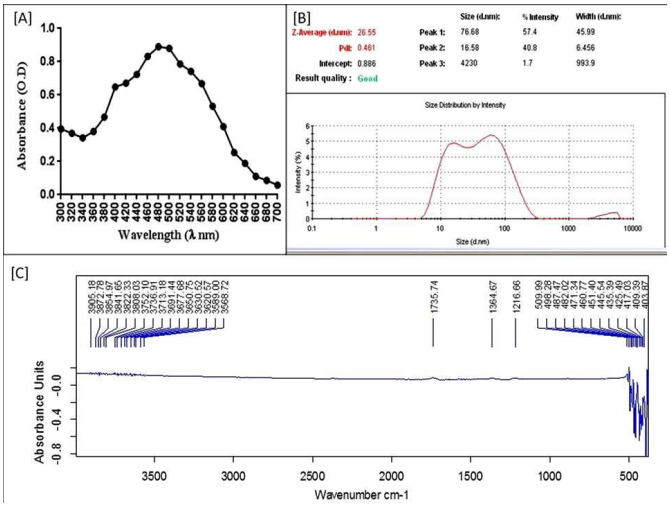

Fig. 2. UV-Vis [**A**]; DLS [**B**] and FTIR [**C**] spectra of Ag-Au BMNPs.

FTIR Spectroscopy results

FTIR analysis was carried out to identify the various functional groups presented on the surface of synthesized nanoparticles, responsible for reducing metallic salts into their respective NPs and their subsequent capping in the solution. AuNPs FTIR spectra showed absorption vibrations at 402-495, 505, 529, 952, 1021, 1222, 1361, 1420, 1706 and

3427 cm^{-1} (Fig. 1C), whereas BMNPs showed absorption peaks at 403-489, 509, 1216, 1364, 1735 and 3568-3905 cm^{-1} (Fig. 2C).

HRTEM/EDX/DLS/Zeta potential results analysis

As shown in Fig. 3 & 4, both AuNPs and Ag-Au BMNPs were

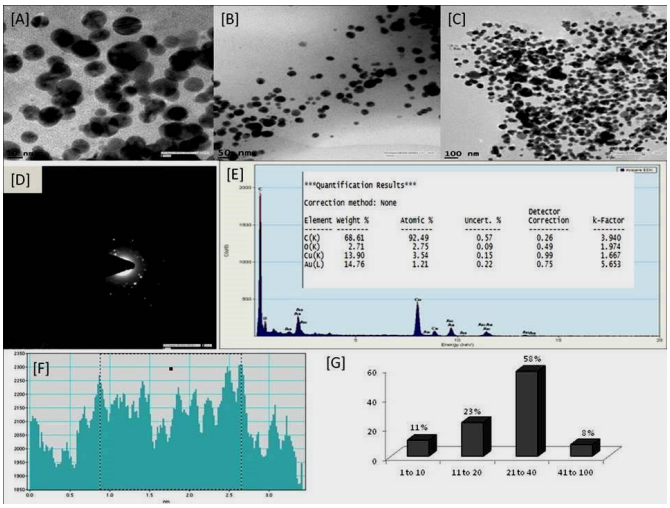

Fig. 3. HRTEM micrograph of AuNPs with scale bar 10 nm [**A**], 50 nm [**B**] and 100 nm. SAED pattern [**D**]; EDX spectra [**E**]; Line profile of lattice fringes [**F**] and histogram [**G**] results of AuNPs.

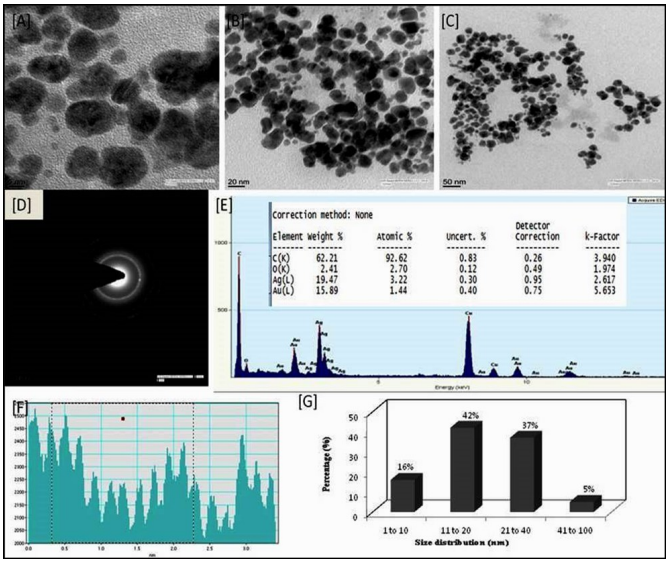

Fig. 4. HRTEM micrograph of Ag-Au BMNPs with scale bar 5 nm [**A**], 20 nm [**B**] and 50 nm. SAED pattern [**D**]; EDX spectra [**E**]; Line profile of lattice fringes [**F**] and histogram [**G**] results of BMNPs.

found to possess mainly spherical morphology along with a low percentage of oval shapes. In case of AuNPs, NPs size was observed in the range of 5 to 40 nm (Fig. 3), which is in justification with the DLS results (average hydro-diameter 29.08 nm) as shown in Fig. 1B. In the case of BMNPs, HRTEM micrograph depicted NPs with size in the range of 5 to 30 nm (Fig. 4), which is again in consonance with DLS results (Fig. 2B) which demonstrated the presence of BMNPs with an average hydro-diameter size of 26.56 nm. Histogram profile was constructed by counting 100 NPs of both AuNPs and BMNPs. As per histogram results, AuNPs size distribution in the profile was found as follows: 1-10 nm (11%), 11-20 (23%), 21-40 (58%) and 41-100 (8%), whereas BMNPs size distribution was: 1-10 nm (16%), 11-20 (42%), 21-40 (37%) and 41-100 (5%) as shown in Fig. 3G & 4G. SAED pattern analysis confirmed the high crystalline nature of both AuNPs and BMNPs, as shown in Fig. 3D & 4D. EDX spectra results showed that in case of AuNPs, Au was the only ingredient metal (14.76 wt %), whereas in case of BMNPs the ingredient metals were Ag (19.47 wt %) and Au (15.89 wt %) as depicted in Fig. 3E & 4E. Lattice profiles of AuNPs and BMNPs are shown in Fig. 3F & 4F, which suggest the average 'd-spacing' of lattice fringes of respective inter-plane distance. Furthermore, in concordance with the FTIR results, which demonstrated the anisotropy of reactions, HRTEM and DLS result also revealed the presence of various sizes of NPs in case of both AuNPs and BMNPs. Moreover, both NPs were well dispersed in the solution, and no agglutination was observed.

Antibacterial potential of synthesized BMNPs and AuNPs

In the case of agar-well diffusion assay, the presence of a clear zone around the agar-well is attributed to restricted bacterial growth and is an evidence of the antibacterial potential of NPs. Agar well diffusion assay results demonstrated that BMNPs possessed profound bactericidal effect against all gram-positive experimental bacterial strains (Fig. 5, Table 1 & 2). At the highest concentration (3mg/ml),

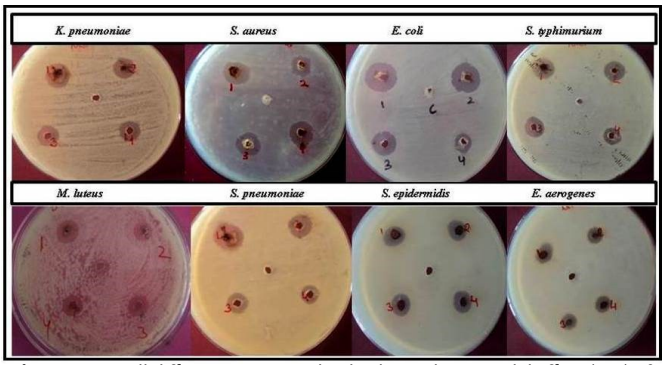

Fig. 5. Agar well diffusion assay results displaying bactericidal effect (ZOI) of Ag-Au BMNPs against gram-positive and gram-negative bacteria.

Table 1. Comparative analysis of ZOI observed against various gram-positive bacteria by different concentrations of AuNPs and BMNPs using agar well diffusion assay

Bacteria	NPs	ZOI (mm±SD)			
		(3.0 mg/ml)	(2.0 mg/ml)	(1.0 mg/ml)	(0.5 mg/ml)
S. aureus	BMNPs	10.83±0.28	8.16±0.28	5.33±0.57	4.16±0.28
	AuNPs	6.83±0.28	3.33±0.57	1.83±0.28	1.33±0.57
M. luteus	BMNPs	9.33±0.57	6.83±0.28	3.83±0.28	3.33±0.57
	AuNPs	6.16±0.28	4.33±0.57	1.16±0.28	NE
S. pneumoniae	BMNPs	8.33±0.57	5.16±0.28	4.33±0.57	3.16±0.28
	AuNPs	4.83±0.28	3.33±0.57	1.83±0.28	NE
S. epidermidis	BMNPs	8.16±0.28	4.83±0.28	3.16±0.28	1.83±0.28
	AuNPs	4.33±0.57	2.16±0.28	NE	NE

Table 2. Comparative analysis of ZOI observed against various gram-negative bacteria by different concentrations of AuNPs and BMNPs using agar well diffusion assay

Bacteria	NPs	ZOI (mm±SD)			
		(3.0 mg/ml)	(2.0 mg/ml)	(1.0 mg/ml)	(0.5 mg/ml)
E. coli	BMNPs	10.33±0.57	7.16±0.28	5.83±0.28	4.16±0.28
	AuNPs	4.83±0.28	4.16±0.28	3.33±0.57	1.33±0.57
S. typhimurium	BMNPs	9.83±0.28	6.33±0.57	4.33±0.57	2.83±0.28
	AuNPs	4.16±0.28	2.83±0.28	1.16±0.28	1.00±0.00

K. pneumoniae	BMNPs	12.33±0.57	9.33±0.57	7.16±0.28	5.33±0.57
	AuNPs	7.33±0.57	5.33±0.57	3.16±0.28	1.83±0.28
E. aerogenes	BMNPs	7.83±0.28	4.16±0.28	2.33±0.57	1.16±0.28
	AuNPs	4.83±0.28	2.33±0.57	1.00±0.00	NE

BMNPs were observed as the most potent bactericidal agent against *S. aureus* (ZOI: 10.83+0.28 mm) followed by *M. luteus* (ZOI: 9.33+0.57 mm)> *S. pneumoniae* (ZOI: 8.33+0.57 mm) and least effective against bacteria *S. epidermidis* (ZOI: 8.16+0.28 mm). In case of gram-negative bacteria, BMNPs demonstrated remarkable bactericidal effect in the order of *K. pneumoniae* (ZOI: 12.33+0.57 mm)> *E. coli* (ZOI: 10.33+0.57 mm)> *S. typhimurium* (ZOI: 9.83+0.28 mm) and *E. aerogenes* (ZOI: 7.83+0.28 mm). Results obtained in XTT-colorimetric assay demonstrated that at the concentration of 1000 µg/ml, BMNPs showed full inhibitory effect (>99.0 %) against all gram-positive bacteria from the present study (Table 3 & 4). BMNPs at the concentration of 800 µg/ml, still possessed complete inhibitory effect against *S. aureus*, *M. luteus* and *S. pneumoniae*. *S. aureus* was found to be the most sensitive gram-positive bacteria which demonstrated complete inhibition up to the concentration of 600 µg/ml (>99.0 %) followed by *M. luteus* (96.55%)> *S. pneumoniae* (94.24)> *S. epidermidis* (91.81%). Furthermore, BMNPs were found to possess promissory bactericidal effect against *S. aureus* (47.67%) up to the concentration of 50 µg/ml, whereas other gram-positive bacteria showed modest bactericidal effect at the same concentration in the order of *S. pneumoniae* (27.57%)> *M. luteus* (17.24%) and *S. epidermidis* (10.76%). All gram-positive bacteria, except *S. aureus* (27.35%) did not show the bactericidal effect at the concentration of 25 µg/ml or less. In case of gram-negative bacteria, as per XTT results (Table 5 & 6), BMNPs exhibited complete inhibitory potential against *K. pneumoniae* up to the concentration of 400 µg/ml. Furthermore, at the concentration of 600 µg/ml, *S. typhimurium* showed complete inhibition followed by *E. aerogenes* (97.66 %) and *E. coli* (95.85%). Up to the concentration of 25 µg/ml, *K. pneumoniae* (20.37%) and *S. typhimurium* (20.44%) demonstrated inhibitory effect, whereas *E. aerogenes* (21.53 %) and *E. coli* (14.63%) exhibited bactericidal effect only up to the concentration of 50 µg/ml.

In case of AuNPs-mediated bactericidal effect against experimental bacteria, it was observed that at the concentration of 3 mg/ml (Fig. 6, Table 1 & 2), AuNPs showed passable bactericidal effect against gram-positive bacteria *S. aureus* (ZOI: 6.83+0.28 mm) followed by *M. luteus* (ZOI: 6.16+0.28 mm)> *S. pneumoniae* (ZOI: 4.83+0.28 mm) and *S. epidermidis* (ZOI: 4.33+0.57 mm). In the case of gram-negative bacteria, the trend of AuNPs-mediated bactericidal effect (3.0 mg/ml) was observed in the order of *K. pneumoniae* (ZOI: 7.33+0.57 mm)> *E. coli* (ZOI: 4.83+0.28 mm)> *E. aerogenes* (ZOI: 4.83+0.28 mm)> *S. typhimurium* (ZOI: 4.16+0.28 mm). As shown in Table 1 & 2, at other lower concentrations, antibacterial effect (ZOI) of AuNPs against experimental bacterial strains follows the similar or slightly different trend of effectiveness. For gram-positive bacteria (Table 3 & 4), it was demonstrated that at the concentration of 1000 µg/ml, *S. aureus* and *S. pneumoniae* showed complete inhibition. Up to the concentration of 100 µg/ml, AuNPs exhibited a passable level of bactericidal effect against bacteria *S. pneumoniae* (35.29%), *S. aureus* (31.69%) and *M. luteus* (28.03%). *S. aureus* was found to be the most sensitive gram-positive bacteria which showed

Table 3. Measurement of O.D of growth (mean±standard deviation) of different gram-positive bacteria at different concentration (µg/ml) of NPs

Bacteria	NPs	PC	NC	1000	800	600	400	200	100	50	25
S.aureus	BMNPs	0.055±0.006	0.837±0.043	0.004±0.002	0.007±0.008	0.008±0.006	0.067±0.009	0.204±0.011	0.317±0.019	0.438±0.018	0.608±0.019
	AuNPs	0.101±0.010	0.751±0.016	0.009±0.001	0.017±0.004	0.075±0.009	0.230±0.026	0.347±0.026	0.513±0.020	0.680±0.011	NE
M.luteus	BMNPs	0.076±0.027	0.725±0.021	0.004±0.004	0.025±0.008	0.081±0.011	0.226±0.022	0.393±0.013	0.600±0.022	NE	NE
	AuNPs	0.080±0.010	0.799±0.018	0.015±0.004	0.081±0.010	0.136±0.008	0.300±0.015	0.421±0.017	0.575±0.018	NE	NE
S.pneumoniae	BMNPs	0.118±0.031	0.816±0.035	0.008±0.003	0.004±0.001	0.047±0.010	0.111±0.014	0.281±0.023	0.412±0.013	0.591±0.017	NE
	AuNPs	0.055±0.005	0.884±0.021	0.004±0.004	0.057±0.005	0.173±0.008	0.290±0.015	0.399±0.025	0.572±0.008	NE	NE
S.epidermidis	BMNPs	0.061±0.020	0.892±0.024	0.008±0.001	0.018±0.007	0.073±0.015	0.161±0.015	0.315±0.016	0.504±0.028	0.7960.016	NE
	AuNPs	0.116±0.011	0.808±0.033	0.022±0.006	0.090±0.016	0.233±0.030	0.475±0.017	0.691±0.014	NE	NE	NE

Table 4. Percentage (%) reduction of gram-positive bacterial growth with respect to NPs concentrations (µg/ml) as per XTT-colorimetric results

Bacteria	NPs	PC	1000	800	600	400	200	100	50	25
S. aureus	BMNPs	93.42	CI	CI	CI	91.99	75.62	62.12	47.67	27.35
	AuNPs	86.55	CI	97.73	90.01	69.37	53.79	31.69	9.45	NE
M. luteus	BMNPs	89.51	CI	CI	96.55	88.82	68.82	45.79	17.24	NE
	AuNPs	89.98	98.12	89.86	82.97	62.45	47.30	28.03	NE	NE
S. pneumoniae	BMNPs	85.53	CI	CI	94.24	86.39	65.56	49.50	27.57	NE
	AuNPs	93.77	CI	93.55	80.42	67.19	54.86	35.29	NE	NE
S. epidermidis	BMNPs	93.16	CI	97.98	91.81	81.95	64.68	43.49	10.76	NE
	AuNPs	85.64	97.27	88.86	71.16	41.21	14.48	NE	NE	NE

inhibition up to the concentration of 50 µg/ml (9.45%), whereas *S. epidermidis* was observed to be the most resistant gram-positive bacteria which demonstrated low-level bactericidal effect only up to the concentration of 200µg/ml (14.48%). AuNPs-mediated inhibition of gram-negative bacteria (Table 5 & 6) revealed that at 1000 µg/ml concentration, there was complete inhibition of all gram-negative bacterial strains. Gram-negative bacteria *S. typhimurium* showed complete inhibition up to the concentration of 800 µg/ml, followed by *E. coli* (97.33%)> *K. pneumoniae* (95.32%)> *E. aerogenes* (88.34%). *S. typhimurium* (15.58 %) and *K. pneumoniae* (9.24%) were found to be the most sensitive gram-negative bacteria which showed inhibition up to the concentration of 50 µg/ml. Whereas, *E. coli* (19.89%) and *E. aerogenes* (20.75%) were calculated to be the most resistant gram-negative bacteria against AuNPs-mediated inhibition up to the concentration of 100 µg/ml and 200 µg/ml respectively.

Table 5. Measurement of O.D of growth (mean±standard deviation) of different gram-negative bacteria at different concentration of NPs

Bacteria	NPs	PC	NC	1000	800	600	400	200	100	50	25
E. coli	BMNPs	0.106±0.030	0.868±0.033	0.005±0.003	0.009±0.002	0.036±0.012	0.099±0.014	0.273±0.058	0.510±0.050	0.741±0.036	NE
	AuNPs	0.048±0.013	0.789±0.022	0.009±0.002	0.021±0.007	0.073±0.016	0.164±0.008	0.399±0.017	0.632±0.022	NE	NE
S. typhimurium	BMNPs	0.084±0.010	0.890±0.013	0.005±0.002	0.006±0.001	0.008±0.003	0.032±0.007	0.120±0.014	0.309±0.017	0.602±0.027	0.708±0.016
	AuNPs	0.043±0.023	0.834±0.046	0.009±0.004	0.009±0.002	0.039±0.017	0.072±0.026	0.306±0.036	0.443±0.048	0.704±0.055	NE
K. pneumoniae	BMNPs	0.056±0.021	0.903±0.041	0.003±0.002	0.006±0.001	0.007±0.003	0.006±0.005	0.031±0.015	0.171±0.062	0.423±0.088	0.719±0.039
	AuNPs	0.098±0.033	0.898±0.020	0.006±0.001	0.042±0.011	0.097±0.010	0.168±0.018	0.283±0.020	0.649±0.026	0.815±0.022	NE
E. aerogenes	BMNPs	0.160±0.028	0.901±0.023	0.004±0.003	0.010±0.002	0.021±0.008	0.093±0.010	0.272±0.025	0.527±0.022	0.707±0.023	NE
	AuNPs	0.064±0.012	0.824±0.062	0.009±0.001	0.096±0.027	0.230±0.031	0.519±0.038	0.653±0.040	NE	NE	NE

Table 6. Percentage (%) reduction of gram-negative bacterial growth with respect to NPs concentrations (µg/ml) as per XTT-colorimetric results

Bacteria	NPs	PC	1000	800	600	400	200	100	50	25
E. coli	BMNPs	87.78	CI	CI	95.85	88.59	68.54	41.24	14.63	NE
	AuNPs	93.91	CI	97.33	90.74	79.21	49.42	19.89	NE	NE
S. typhimurium	BMNPs	90.56	CI	CI	CI	96.40	86.51	65.28	32.35	20.44
	AuNPs	94.84	CI	CI	95.32	91.36	63.30	46.88	15.58	NE
K. pneumoniae	BMNPs	93.79	CI	CI	CI	CI	96.56	81.06	53.15	20.37
	AuNPs	89.08	CI	95.32	89.19	81.29	68.48	27.72	9.24	NE
E. aerogenes	BMNPs	82.24	CI	CI	97.66	89.67	69.81	41.50	21.53	NE
	AuNPs	92.23	CI	88.34	72.08	37.01	20.75	NE	NE	NE

Discussion

Literature showed that different labs synthesized spherical AuNPs of various sizes (5-200 nm) using leaf extract of *Zingiber officinale* (31), *Hibiscus rosa sinensis* (32), aqueous seed extract of *Abelmoschus esculentus* (33), buds of *Syzygium aromaticum* (34) etc. Similarly, BMNPs were phytofabricated in size range of 5-150 nm using different plants such as leaf extract of *Piper betel* (35), *Plumbago zeylanica* (36), *Gloriosa superba* (37), *Antigonon leptopus* (38), Chinese wolfberry fruit extract (39) and many other plants (8, 40). Aqueous leaf extract of *Triticum aestivum* L. contains various phytochemicals which have high potential to reduce silver and gold ions into their respective NPs. As per literature, reduction reactions involving the production of AuNPs and Ag-Au BMNPs using plants extract were generally found to be completed within 5-30 min (37, 41). It has been proposed that formation of NPs is a two-step process: First, there is a reduction of Au^{3+}/Ag^{+1} ions (soluble cations) into Au^{0}/Ag^{0} (insoluble metal atoms), followed by the second step which involved an aggregation process of these reduced metal atoms. The method of NPs production was performed in standard conditions of temperature (90+1.0 ^{0}C), pH (10.0+0.2), lower concentration of precursor salts and high concentration of reducing agent. This is because of the reason that at the lower concentration of precursor salt, the diffusion of gold and silver atoms on the surface of the nanoparticles takes place slowly and directionally. Second, high pH, temperature and high concentration of reducing agent help the number of particles with enough energy to overcome the critical energy barrier and make the reaction fast (1, 11, 18). The obtained results justify the earlier reports which confirm the influence of standardized reduction procedure on the production of small size NPs, and their UV-Visible spectroscopic characteristics like the spectral peaks in the range of 420-495 nm for BMNPs and 520-540 nm in case of AuNPs (42). In the present study, both NPs were mostly spherical with some percentage of oval-shaped nanoparticles and these shapes are best suited for biomedical applications (43).

The FTIR spectrum of AuNPs showed the absorption peak at 1021 cm^{-1} which was due to the -C-O- stretching vibrations of anhydroglucose ring (15, 44-46). Peaks at 1361 (AuNPs) and 1364 cm^{-1} (BMNPs) were ascribed to the

stretching vibration of =C=O- bond of water-soluble compounds flavonoids or terpenoids (40). Bands at 1216 (BMNPs) and 1222 cm^{-1} (AuNPs) were found to be the characteristics of Amide III bands of proteins (39). Peaks at 1706 (AuNPs) cm^{-1} and 1735 (BMNPs) cm^{-1} were ascribed to C-O stretching vibration of carboxylic acid (-COOH) groups (30, 46, 47). A band at 1420 cm^{-1} (AuNPs) was observed due to the presence of in-plane bending of C-H (wagging of CH_2 and CH_3) group (7, 44, 46, 48). Peaks in the range of 3427-3671 cm^{-1} (BMNPs) comprises of O-H stretching vibration of alcohol/phenol group (49). Furthermore, peaks in the range of 3713-3905 cm^{-1} (BMNPs) were attributed to adsorbed moisture present in synthesized NPs (18). Above-mentioned functional groups on NPs prevent agglomeration of the nanoparticles and their stabilization in the aqueous solvent. A band at 952 cm^{-1} (AuNPs) was ascribed to out-of-plane deformation vibrations of –COOH group (39). In the plant-mediated synthesis of NPs, observation of bands in the range of 400- 530 cm^{-1} was mainly ascribed to stretching vibrations of the polyaromatic system and indicated the success of the reaction and formation of NPs (18, 25, 50, 51). Moreover, presence of multiple bands, especially between 400-450 cm^{-1} in the FTIR spectra of both NPs, suggests that particle size was significantly varying because of anisotropy existing in the reaction outcome (52). Overall, FTIR results demonstrated that proteins, aromatic amines, reducing sugars and polyphenols were acted as both reducing and capping agents in phytofabrication and stabilization of NPs. Several studies demonstrated that water-soluble flavonoid, phenolics compounds, alkaloids, proteins and reducing sugars present in plants are accountable for the formation of NPs and their stabilization in the solution (18, 25, 38, 41, 53).

Results from previous studies unanimously agreed on the fact that BMNPs have a more profound bactericidal effect than that of AuNPs. It was demonstrated that BMNPs showed ZOI against *S. aureus* (9.0+0.1 mm), *E. coli* (15.0+0.2 mm), *P. aeruginosa* (9.0+0.1 mm) and *M. luteus* (13.0+0.2 mm) (54). It was also revealed a modulatory bactericidal effect of BMNPs against *S. aureus* (7.65+0.28 mm), *M. luteus* (8.12+0.4 mm) and *S. epidermis* (8.0+0.1 mm) (16). Similarly, it was showed that BMNPs produced profound inhibitory effect against *B. subtilis* (14.66+0.57 mm), *E. coli* (11.0+1.0 mm), *S. typhimurium* (9.33+1.52 mm) and *S. aureus* (13.66+0.57 mm) (55). In some studies, the concentration-dependent bactericidal effect of BMNPs was demonstrated. For example, BMNPs exhibited remarkable ZOI against *B. cereus* (21.0 mm), *E. coli* (17.0 mm), *B. subtilis* (24.0 mm) and *P. aeruginosa* (20.0mm) at the concentration of 100 µg/ml (56). Similarly, reports are on demonstrated the concentration-dependent significant bactericidal effect against *S. aureus* (18.0 mm) and *E. coli* (20.0 mm) (57). In the present study, BMNPs showed excellent inhibitory potential against both kinds of bacteria in a concentration-dependent manner, as discussed in previous sections.

Reports are on the evaluation of MIC values of BMNPs against bacteria *S. aureus* and *E. coli,* and it was found to be 85 and 95 µg/l respectively (57). It was also observed that there are very low MIC values of BMNPs against *S. aureus* (3 µg/ml) and *E. coli* (6 µg/ml) (46). Whereas, reports are on the MIC values in the range of 16, 4 and 8µg/well against *A. baumanni*, *E. coli* and *S. aureus* respectively (36). In the same study, chemically synthesized BMNPs showed MIC values in the range of 256, 32 and 512 µg/well against *A. baumanni*, *E. coli* and *S. aureus* respectively. It was revealed that the MIC values against *E. coli*, *P. aeruginosa*, *E. facaelis* and *S. aureus* in the range of 25-50µM (15). In the present study, the results revealed that both MIC and MBC (BMNPs) values were estimated in the range of 400µg/ml for bacteria *K. pneumoniae*, 600µg/ml for bacteria *S. typhimurium* and *S. aureus*. In case of *S. pneumoniae*, *M. luteus*, *E. coli* and *E. aerogenes* both MIC and MBC values were found in the range of 800µg/ml and in case of *S. epidermidis* values were observed to be 1000 µg/ml.

In case of AuNPs, it was revealed that bactericidal activity is not one of the inherent characteristics of AuNPs owing to their property of being biologically inert. Although, in literature, there is an ambiguity with regards to their antibacterial potential. Importantly, it has been demonstrated that plant-mediated synthesized AuNPs showed antibacterial potential against diverse kinds of pathogenic bacteria, but not the chemically or physically synthesized AuNPs. It was proposed that these differences may be due to the presence of biologically active molecules or functional groups (from plants) on AuNPs, which facilitates their proper attachment to the bacterial membrane and hence improved their antibacterial activity. For example, It was demonstrated that phytosynthesized AuNPs at the concentration of 1.25 mg/ml showed profound inhibition zone against *B. cereus* (11.1 mm), *S. aureus* (11.4 mm), *P. aeruginosa* (15.4 mm) and *E. coli* (14.7 mm) (41). Some more studies further observed concentration-dependent bactericidal efficacy of AuNPs. It was also demonstrated that AuNPs in the concentration range of 50-300 µg/ml exhibited good zone of inhibition against *B. subtilis* (15.33+0.57 to 20.01+0.01) and *E. coli* (12.00+0.57 to 16.66+0.57) (58). Similarly, AuNPs were observed to exert bactericidal effect against *S. aureus* (10.0 to 30.0 mm) and *E. coli* (16.0 to 25.0 mm) at the concentration of 100-200 µg/ml (50). In the liquid media, AuNPs (200 µg/ml) reduced the growth of *S. aureus* (91.8%) and *E. coli* (20.0%) (50). It is now almost clear that the bactericidal effect of AuNPs is strongly correlated with the dose of administration. As shown in our results, we have also observed the concentration-dependent (>100 µg/ml) AuNPs inhibitory effect against the experimental bacterial strains.

Hand full of literature is available on AuNPs-mediated MIC inhibition studies. MIC was found to be 100 µg/l and 105 µg/l against *S. aureus* and *E. coli* respectively (5) and 128, 256 and 8 µg/well against *A. baumanni*, *E. coli* and *S. aureus* respectively (36). Reports are on the evaluation of the MIC values as >182 µg/ml against *E. coli* and *P. aeruginosa* (59), whereas, calculations are on the MIC values in the range of 12.5 and 25 µg/ml against *E. coli* and *S. aureus* respectively (30). MIC and MBC values of AuNPs were estimated against all the experimental bacteria in the pre-

sent study. MIC and MBC values were observed in the range of 800µg/ml for *S. typhimurium*, and 1.5mg/ml for *S. epidermidis* and *M. luteus*. For all other remaining bacterial strains, 1000 µg/ml concentration was recorded as both MIC and MBC value.

Several studies demonstrated that BMNPs kill bacteria through the reactive oxygen species (ROS)-mediated killing mechanism (60), whereas, some other studies exhibited that the BMNPs-mediated killing involves the formation of irreparable pores on the bacterial cell membrane which caused bacterial cell lysis. Recently, it has been postulated that BMNPs damage actin cytoskeleton protein "MreB" of bacteria *Bacillus subtilis* which resulted in fluidization of inner bacterial membrane and ultimately resulted in the death of bacterial cells (61). One of the mechanisms involving the bactericidal effect of AuNPs showed that first of all coulomb potential-mediated AuNPs adsorption took place on the bacterial lipid surface, which resulted in decompression of lipid bilayer. Then due to dipole-charge, phosphocholine on the bacterial membrane changes its position from inclined to a vertical position which resulted in irreparable pore formation and death of bacteria (62). Inside the cell, Ag and Au ions exert their bactericidal effect by interacting and damaging the sulfur- and phosphorous-containing cellular components of bacterial cells (15, 63). BMNPs have both metals *i.e.* silver and gold, and this is obvious that the bactericidal effect of BMNPs is a synergistic outcome of antibacterial potential of both the metals. Overall, the bactericidal effect of both AuNPs and BMNPs depends on several factors like size, shape, dose-concentrations, diffusivity, stability, releasing of ions in the solution from NPs surface, functional groups immobilized on NPs and type of experimental bacterial strains.

Currently, humankind is living in a low-efficacy and resistant era of antibiotics which pose a survival threat to humanity. As per the report of CDC (Centers for Disease Control and Prevention), if this menace of resistance in microbes is not prevented, then it could be responsible for more than 10 million deaths and loss of 100 trillion dollars (USD) worldwide by the year 2050 (64). Therefore, microbiologists are involved in isolation and designing of new effective antibacterial compounds alone or in conjugation with antibiotics or other effective molecules to combat pathogenic and life-threatening bacterial infections. Phytosynthesized AuNPs and BMNPs appear as a potential answer to this problem. In the case of AuNPs, their well-tunable SPR effect and photothermal property make them an excellent candidate to fight against bacterial infections. On the other hand, in case of bimetallic Ag/Au alloy NPs, it is possible to vary their individual metallic compositions systematically and to produce different kind of shapes (e.g. sharp edges or protrusions), and sizes which have profound antibacterial activity as well as have excellent biocompatibility towards human cells and tissues (6).

Conclusion

Phytosynthesis of AuNPs and Ag-Au BMNPs deserve invaluable merit due to its highly reproducible, sustainable, biocompatible and easy to scale up potentials. In the present study, crop plant *Triticum aestivum* leaves were used to fabricate AuNPs and BMNPs and were evaluated for their bactericidal potential. As discussed in the introduction, there remains ambiguity regarding the bactericidal effect of both AuNPs and BMNPs (Ag-Au NPs) in literature. Our study demonstrated that phytosynthesized AuNPs have their own bactericidal efficiency, but at higher concentrations (dose-dependent) and also found to be different for different bacterial strains. Furthermore, as size and shape of both NPs are in the same range, and also the functional groups on both the NPs are similar, we, on the basis of bactericidal results, can conclude that antibacterial potential of Ag-Au BMNPs was due to the synergistic effect of both ingredient metals *i.e.* Ag and Au. These NPs can be easily manipulated on their functional groups to improve their specificity, sensitivity and functionality through surface modifications like addition, immobilization or conjugation with specific ligands as per laboratory requirements. Moreover, this eco-friendly, highly reproducible and environment benign fabrication method is crop-plant based, which remains an inexhaustible resource as compared to other plant species.

Acknowledgements

The authors would like to thank National Institute of Pharmaceutical Education and Research, (NIPER), SAS Nagar, Mohali, Punjab (India) and Bio-Nanotechnology Lab, Central Scientific Instruments Organization (CSIO), Chandigarh (U.T), India for analyzing the nanoparticles for their physical attributes. We extend our gratitude to Dolphin (PG) college of Science and Agriculture for providing necessary facilities for carrying out the experiments.

Authors contributions

VP conceived and designed the research. VP and PG conducted all the experiments. PK and VK analyzed the physical attributes of nanoparticles using various analytical tools. VP analyzed the data and performed the experimental result analysis and wrote the final manuscript. All authors read and approved the final manuscript.

Compliance with ethical standards

Conflict of interest: The authors declare that they have no conflict of interest.

Ethical issues: This article does not contain any studies with human participants or animals performed by the authors.

References

1. Baker S, Pasha A, Satish S. Biogenic nanoparticles bearing antibacterial activity and their synergistic effect with broad spectrum antibiotics: Emerging strategy to combat drug resistant pathogens. Saudi Pharm J. 2017;25(1):44-51. https://doi.org/10.1016/j.jsps.2015.06.011

2. Weng Y, Li J, Ding X, Wang B, Dai S, Zhou Y, Pang R, Zhao Y, Xu H, Tian B, Hua Y. Functionalized gold and silver bimetallic nanopar-

ticles using *Deinococcus radiodurans* protein extract mediate degradation of toxic dye malachite green. Int J Nanomedicine. 2020;16(15):1823-35. https://doi.org/10.2147/IJN.S236683

3. Tao C. Antimicrobial activity and toxicity of gold nanoparticles: research progress, challenges and prospects. Lett Appl Microbiol. 2018; 67(6):537-43. https://doi.org/10.1111/lam.13082
4. Tang Y, Xu J, Xiong C, Xiao Y, Zhang X, Wang S. Enhanced electrochemiluminescence of gold nanoclusters *via* silver doping and their application for ultrasensitive detection of dopamine. Analyst. 2019;144(8):2643-48. https://doi.org/10.1039/C9AN00032A
5. Lopez-Miranda JL, Esparza R, Rosas G, Pérez R, Estévez-González M. Catalytic and antibacterial properties of gold nanoparticles synthesized by a green approach for bioremediation applications. 3 Biotech. 2019; 9(4):135. https://doi.org/10.1007/s13205-019-1666-z
6. Penders J, Stolzoff M, Hickey DJ, Andersson M, Webster TJ. Shape-dependent antibacterial effects of non-cytotoxic gold nanoparticles. Int J Nanomed. 2017;12:2457-68. https://doi.org/10.2147/IJN.S124442
7. Ahmed F, Faisal SM, Ahmed A, Husain Q. Beta galactosidase mediated bio-enzymatically synthesized nano-gold with aggrandized cytotoxic potential against pathogenic bacteria and cancer cells. J Photochem Photobiol B. 2020;209:111923. https://doi.org/10.1016/j.jphotobiol.2020.111923
8. Nasrabadi HT, Abbasi E, Davaran S, Kouhi M, Akbarzadeh A. Bimetallic nanoparticles: Preparation, properties and biomedical applications. Artif Cells Nanomed Biotechnol. 2016;44(1):376-80. https://doi.org/10.3109/21691401.2014.953632
9. Pathak PK, Kumar A, Prasad BB. Functionalized nitrogen doped graphene quantum dots and bimetallic Au/Ag core-shell decorated imprinted polymer for electrochemical sensing of anticancerous hydroxyurea. Biosens Bioelectron. 2019;127:10-18. https://doi.org/10.1016/j.bios.2018.11.055
10. Yaseen T, Pu H, Sun DW. Rapid detection of multiple organophosphorus pesticides (triazophos and parathion-methyl) residues in peach by SERS based on core-shell bimetallic Au@Ag NPs. Food Addit Contam Part A Chem Anal Control Expo Risk Assess. 2019;36(5):762-78. https://doi.org/10.1080/19440049.2019.1582806
11. Reddy PB, K Mallikarjuna GN, Si-Hyun P. *Plectranthus amboinicus* -mediated silver, gold, and silver-gold nanoparticles: phytosynthetic, catalytic and antibacterial studies. Mat Res Exp. 2017; 4:085010. https://doi.org/10.1088/2053-1591/aa80a2
12. Arora N, Thangavelu K, Karanikolos GN. Bimetallic Nanoparticles for Antimicrobial Applications. Front Chem. 2020;8:412. https://doi.org/10.3389/fchem.2020.00412
13. Yaqoob SB, Adnan R, Rameez Khan RM, Rashid M. Gold, silver and palladium nanoparticles: A chemical tool for biomedical applications. Front Chem. 2020;8:376. https://doi.org/10.3389/fchem.2020.00376
14. Baker S, Nagendra PMN, Chouhan RS, Mohan KK, Satish S. Development of bioconjugated nano-molecules against targeted microbial pathogens for enhanced bactericidal activity. Mater Chem Phys. 2020;242:122292. https://doi.org/10.1016/j.matchemphys.2019.122292
15. Ramasamy M, Lee JH, Lee J. Potent antimicrobial and antibiofilm activities of bacteriogenically synthesized gold-silver nanoparticles against pathogenic bacteria and their physiochemical characterizations. J Biomater Appl. 2016;31(3):366-78. https://doi.org/10.1177/0885328216646910
16. Chakravarty I, Narasimha P, Singh S, Kundu K, Singh P, Kundu S. Synergistic oligodynamic effect of mycogenic bimetallic nanoparticles with daptomycin for controlling pathogens. Int J Pharm Sci Res. 2018;9(5):1788-96. https://doi.org/10.13040/IJPSR.0975-8232.9(5).1788-96
17. Dahoumane SA, Wijesekera K, Filipe CD, Brennan JD. Stoichiometrically controlled production of bimetallic Gold-Silver alloy colloids using micro-alga cultures. J Colloid Interface Sci. 2014;416:67-72. https://doi.org/10.1016/j.jcis.2013.10.048
18. Singh P, Pandit S, Garnæs J, Tunjic S, Mokkapati VR, Sultan A et al. Green synthesis of gold and silver nanoparticles from *Cannabis sativa* (industrial hemp) and their capacity for biofilm inhibition. Int J Nanomed. 2018;21(13):3571-91. https://doi.org/10.2147/IJN.S157958
19. Tran CD, Prosenc F, Franko M. Facile synthesis, structure, biocompatibility and antimicrobial property of gold nanoparticle composites from cellulose and keratin. J Coll Inter Sci. 2018;510:237-45. https://doi.org/10.1016/j.jcis.2017.09.006
20. Barrett TC, Mok WWK, Murawski AM, Brynildsen MP. Enhanced antibiotic resistance development from fluoroquinolone persisters after a single exposure to antibiotic. Nat Commun. 2019;101177. https://doi.org/10.1038/s41467-019-09058-4
21. Bakkeren E, Diard M, Hardt WD. Evolutionary causes and consequences of bacterial antibiotic persistence. Nat Rev Microbio. 2020. https://doi.org/10.1038/s41579-020-0378-z
22. Sanchez-Lopez E, Gomes D, Esteruelas G, Bonilla L, Lopez-Machado AL, Galindo R, Cano A, Espina M, Ettcheto M, Camins A, Silva AM, Durazzo A, Santini A, Garcia ML, Souto EB. Metal-based nanoparticles as antimicrobial agents: An overview. Nanomater. 2020;292(10):1-39. https://doi.org/10.3390/nano10020292
23. Murali M, Raj MA, Akhil SA, Liji RS, Kumar SS, Nair AM, Kumar NS. Preliminary phytochemical analysis of Wheat grass leaf extracts. Int J Pharm Sci Rev Res. 2016;40(1):307-12.
24. Suriyavathana M, Roopavathi I, Vijayan V. Phytochemical characterization of *Triticum aestivum* (Wheat grass). J Pharmaco Phytochem. 2016;5(1):283-86.
25. Hamouda RA, Hussein MH, Abo-Elmagd RA, Bawazir SS. Synthesis and biological characterization of silver nanoparticles derived from the cyanobacterium *Oscillatoria limnetica*. Sci Rep. 2019;9(1):13071. https://doi.org/10.1038/s41598-019-49444-y
26. Lehrer RI, Rosenman M. Ultrasensitive assays for endogenous antimicrobial polypeptides. J Microbio Met. 1991;137:167-73. https://doi.org/10.1016/0022-1759(91)90021-7
27. Pahal V, Kaur A, Dadhich KS. Effect of combination therapy using cow (*Bos indicus*) urine distillate and some indian medicinal plants against selective pathogenic gram-negative bacteria. Int J Pharm Sci Res. 2017;8(5):2134-42. http://dx.doi.org/10.13040/IJPSR.0975-8232.8 (5).2134-42
28. Al-Bakri GA, Afifi FU. Evaluation of antimicrobial activity of selected plant extracts by rapid XTT colorimetry and bacterial enumeration. J Microbio Met. 2007;68:19-25. https://doi.org/10.1016/j.mimet.2006.05.013
29. Xiu ZM, Zhang QB, Puppala HL, Colvin VL, Alvarez PJ. Negligible particle-specific antibacterial activity of silver nanoparticles. Nano Lett. 2012;12:4271–75. https://doi.org/10.1021/nl301934w
30. Shikha S, Chaudhuri SR, Bhattacharyya MS. Facile one pot greener synthesis of sophorolipid capped gold nanoparticles and its antimicrobial activity having special efficacy against gram negative *Vibrio cholerae*. Sci Rep. 2020;10(1):1463. https://doi.org/10.1038/s41598-019-57399-3
31. Kumar KP, Paul W, Sharma CP. Green synthesis of gold nanoparticles with *Zingiber officinale* extract: Characterization and blood compatibility. Process Biochem. 2011; 46: 2007-13. https://doi.org/10.1016/j.procbio.2011.07.011
32. Philip D. Green synthesis of gold and silver nanoparticles using *Hibiscus rosa- sinensis*. J Physica E**.** 2010;42:1417-24. https://doi.org/10.1016/j.physe.2009.11.081

33. Jayaseelan C, Ramkumar R, Abdul A, Perumal P. Green synthesis of gold nanoparticles using seed aqueous extract of *Abelmoschus esculentus* and its antifungal activity. Ind Crop Prod. 2013;45:423-29. https://doi.org/10.1016/j.indcrop.2012.12.019

34. Raghunandan D, Bedre MD, Basavaraja S, Sawle B, Manjunath SY, Venkataraman A. Rapid biosynthesis of irregular shaped gold nanoparticles from macerated aqueous extracellular dried clove buds (*Syzygium aromaticum*) solution. Coll Surf B Biointerf. 2010;79(1):235-40. https://doi.org/10.1016/j.colsurfb.2010.04.003

35. Lagashetty A, Ganiger SK, Shashidhar. Synthesis, characterization and antibacterial study of Ag-Au Bi-metallic nanocomposite by bioreduction using *Piper betle* leaf extract. Heliyon. 2019;5 (12):e02794. https://doi.org/10.1016/j.heliyon.2019.e02794

36. Salunke GR, Ghosh S, Santosh Kumar RJ et al. Rapid efficient synthesis and characterization of silver, gold and bimetallic nanoparticles from the medicinal plant *Plumbago zeylanica* and their application in biofilm control. Int J Nanomedicine. 2014; 9:2635-53. https://doi.org/10.2147/IJN.S59834

37. Gopinath K, Kumaraguru S, Bhakyaraj K, Mohan S, Venkatesh KS, Esakkirajan M et al. Green synthesis of silver, gold and silver/gold bimetallic nanoparticles using the *Gloriosa superba* leaf extract and their antibacterial and antibiofilm activities. Microb Pathog. 2016;101:1-11. https://doi.org/10.1016/j.micpath.2016.10.011

38. Ganaie SU, Tasneem A, Abbasi SA. Rapid and green synthesis of bimetallic Au–Ag nanoparticles using an otherwise worthless weed *Antigonon leptopus*, J Exp Nanosci. 2016;11:6:395-417. https://doi.org/10.1080/17458080.2015.1070311

39. Li S, Yuechao Y, pengcheng L, Wenxian S, Lixin Z. Green controllable synthesis of Au–Ag alloy nanoparticles using Chinese wolfberry fruit extract and their tunable photocatalytic activity. RSC Adv. 2018;8:3964 -73. https://doi.org/10.1039/C7RA13650A

40. Meena KM, Jacob J, Philip D. Green synthesis and applications of Au-Ag bimetallic nanoparticles. Spectrochim Acta A Mol Biomol Spectrosc. 2015;137:185-92. https://doi.org/10.1016/j.saa.2014.08.079

41. Katas H, Lim CS, Nor Azlan AYH, Buang F, Mh Busra MF. Antibacterial activity of biosynthesized gold nanoparticles using biomolecules from *Lignosus rhinocerotis* and chitosan. Saudi Pharm J. 2019;27(2):283-92. https://doi.org/10.1016/j.jsps.2018.11.010

42. Lomeli-Marroquín D, Medina Cruz D, Nieto-Argüello A, Vernet Crua A, Chen J, Torres-Castro A et al. Starch-mediated synthesis of mono- and bimetallic silver/gold nanoparticles as antimicrobial and anticancer agents. Int J Nanomed. 2019;27(14):2171-90. https://doi.org/10.2147/IJN.S192757

43. Agnihotri S, Mukherji S, Mukherji S. Size-controlled silver nanoparticles synthesized over the range 5–100 nm using the same protocol and their antibacterial efficacy. RSC Adv. 2014;4: 3974–83. https://doi.org/10.1039/C3RA44507K

44. Singh P, Pandit S, Beshay M, Mokkapati VRSS, Garnaes J, Olsson ME et al. Anti-biofilm effects of gold and silver nanoparticles synthesized by the *Rhodiola rosea* rhizome extracts. Artif Cells Nanomed Biotechnol. 2018b; 46(sup3):S886-S899. https://doi.org/10.1080/21691401.2018.1518909

45. Anwar A, Masri A, Rao K, Rajendran K, Khan NA, Shah MR, Siddiqui R. Antimicrobial activities of green synthesized gums-stabilized nanoparticles loaded with flavonoids. Sci Rep. 2019; 9 (1):3122. https://doi.org/10.1038/s41598-019-39528-0.

46. Kumar S, Majhi RK, Singh A, Mishra M, Tiwari A, Chawla S et al. Carbohydrate-Coated Gold-Silver Nanoparticles for Efficient Elimination of Multidrug Resistant Bacteria and *in vivo* Wound Healing. ACS Appl Mater Interf. 2019;11(46):42998-43017. https://doi.org/10.1021/acsami.9b17086

47. Singh R, Nawale L, Arkile M, Wadhwani S, Shedbalkar U, Chopade S et al. Phytogenic silver, gold and bimetallic nanoparticles as novel antitubercular agents. Int J Nanomed. 2016;4(11):1889-97. https://doi.org/10.2147/IJN.S102488

48. Shankar SS, Ahmad A, Pasricha R, Sastry M. Bioreduction of chloroaurate ions by geranium leaves and its endophytic fungus yields gold nanoparticles of different shapes. J Mater Chem. 2003;13:1822. https://doi.org/10.1039/b303808b

49. Rao Y, Inwati GK, Singh M. Green synthesis of capped gold nanoparticles and their effect on Gram-positive and Gram-negative bacteria. Fut Sci OA. 2017; 3(4):FSO239. https://doi.org/10.4155/fsoa-2017-0062

50. Moustafa NE, Alomari AA. Green synthesis and bactericidal activities of isotropic and anisotropic spherical gold nanoparticles produced using *Peganum harmala* L leaf and seed extracts. Biotechnol Appl Biochem. 2019; 66(4):664-72. https://doi.org/10.1002/bab.1782

51. Qais QFA, Shafiq A, Khan HM, Husain FM, Khan RA, Alenazi B et al. Antibacterial effect of silver nanoparticles synthesized using *Murraya koenigii* (L.) against multidrug-resistant pathogens. Bioinorg Chem Appl. 2019; 4649506:1-12. https://doi.org/10.1155/2019/4649506

52. Amerkhanova SK, Shlyapov RM, Afanas'ev DA, Uali AS. The optical and sorption properties of films of polyvinyl alcohol with silver nanoparticles. Plastiche Mas. 2012; 3:12-14.

53. Folorunso A, Akintelu S, Oyebamiji, AK, Ajayi S, Abiola B, Abdusalam I, Morakinyo A. Biosynthesis, characterization and antimicrobial activity of gold nanoparticles from leaf extracts of *Annona muricata*. J Nanostruct Chem. 2019; 9:111-17. https://doi.org/10.1007/s40097-019-0301-1

54. Fakhri A, Tahami S, Naji M. Synthesis and characterization of core -shell bimetallic nanoparticles for synergistic antimicrobial effect studies in combination with doxycycline on burn specific pathogens. J Photochem Photobiol B. 2017;169:21-26. https://doi.org/10.1016/j.jphotobiol.2017.02.014

55. Syed B, Karthik N, Bhat P, Bisht N, Prasad A, Satish S, Nagendra PMN. Phyto-biologic bimetallic nanoparticles bearing antibacterial activity against human pathogens. King Saud Uni Sci. 2019;31:798-803. https://doi.org/10.1016/j.jksus.2018.01.008

56. Bankura K, Maity D, Mollick MR, Mondal D, Bhowmick B, et al. Antibacterial activity of Ag-Au alloy NPs and chemical sensor property of AuNPs synthesized by dextran. Carbohydr Polym. 2014; 107:151-57. https://doi.org/10.1016/j.carbpol.2014.02.047

57. Ahmed HB, Attia MA, El-Dars FMSE, Emam HE. Hydroxyethyl cellulose for spontaneous synthesis of antipathogenic nanostructures: (Ag & Au) nanoparticles versus Ag-Au nano-alloy. Int J Biol Macromol. 2019;128:214-29. https://doi.org/10.1016/j.ijbiomac.2019.01.093

58. Sharma M, Monika, Thakur P, Saini RV, Kumar R, Enza Torino E. Unveiling antimicrobial and anticancerous behavior of AuNPs and AgNPs moderated by rhizome extracts of *Curcuma longa* from diverse altitudes of Himalaya. Sci Rep. 2020;10:10934. https://doi.org/10.1038/s41598-020-67673-4

59. Enrique MA, Guillermina FF, Ocampo-García BE, López-Téllez G, López-Ortega J, Rogel-Ayala DG, Sánchez-Padilla D. Antibacterial efficacy of gold and silver nanoparticles functionalized with the Ubiquicidin (29–41) antimicrobial peptide. J Nanomat Article. 2017; ID 5831959. https://doi.org/10.1155/2017/5831959

60. Alti D, Veeramohan Rao M, Rao DN, Maurya R, Kalangi SK. Gold-silver bimetallic nanoparticles reduced with herbal leaf extracts induce ROS-mediated death in both promastigote and amastigote stages of *Leishmania donovani*. ACS Omega. 2020; 5 (26):16238-45. https://doi.org/10.1021/acsomega.0c02032

61. Jena P, Bhattacharya M, Bhattacharjee G, Satpati B, Mukherjee P, Senapati D, Srinivasan R. Bimetallic gold-silver nanoparticles mediate bacterial killing by disrupting the actin cytoskeleton

MreB. Nanoscale. 2020;12:3731-49. https://doi.org/10.1039/C9NR10700B

62. Ortiz-Benítez EA, Velázquez-Guadarrama N, Durán Figueroa NV, Quezada H, Olivares-Trejo JJ. Antibacterial mechanism of gold nanoparticles on *Streptococcus pneumoniae.* Metallomics. 2019;11(7):1265-76. https://doi.org/10.1039/c9mt00084d

63. Zhang Y, Shareena Dasari TP, Deng H, Yu H. Antimicrobial Activity of Gold Nanoparticles and Ionic Gold. J Environ Sci Health C Environ Carcinog Ecotoxicol Rev. 2015;33(3):286-327. https://doi.org/10.1080/10590501.2015.1055161

64. Yang P, Pageni P, Rahman MA, Bam M, Zhu T, Chen YP et al. Gold nanoparticles with antibiotic-metallopolymers toward broad-spectrum antibacterial effects. Adv Health C Mater. 2019; 8 (6):e1800854. https://doi.org/10.1002/adhm.201800854

§§§